

Supporting Information

Synthesis, Structure, and Spin Crossover Above Room Temperature of a Mononuclear and Related Dinuclear Double Helicate Iron(II) Complexes

Hiroaki Hagiwara,^{*a} Tomoko Tanaka^a and Shiori Hora^b

^a Department of Chemistry, Faculty of Education, Gifu University, Yanagido 1-1, Gifu 501-1193, Japan

^b Graduate School of Education, Gifu University, Yanagido 1-1, Gifu 501-1193, Japan

Table of Contents

Fig. S1 TG/DTA curves of $[\text{Fe}^{\text{II}}(\text{L1}^{\text{Me}})_2](\text{PF}_6)_2$ (1)	S2
Fig. S2 TG/DTA curves of $[\text{Fe}^{\text{II}}_2(\text{L2}^{\text{C}2})_2](\text{PF}_6)_4 \cdot 5\text{H}_2\text{O} \cdot \text{MeCN}$ (2)	S2
Fig. S3 The magnetic behaviour of desolvated sample 2' in the form of the $\chi_M T$ vs. T plots.	S3
Fig. S4 Heterochiral 2D structure of $[\text{Fe}^{\text{II}}(\text{L1}^{\text{Me}})_2](\text{PF}_6)_2$ (1) at 150 K	S3
Fig. S5 Heterochiral 2D layer of $[\text{Fe}^{\text{II}}_2(\text{L2}^{\text{C}2})_2](\text{PF}_6)_4 \cdot 5\text{H}_2\text{O} \cdot \text{MeCN}$ (2) at 120 K	S4
Fig. S6 PXRD patterns of 2 at room temperature in different states	S4
Table S1 X-ray Crystallographic Data for $[\text{Fe}^{\text{II}}(\text{L1}^{\text{Me}})_2](\text{PF}_6)_2$ (1) at 150 and 448 K and $[\text{Fe}^{\text{II}}_2(\text{L2}^{\text{C}2})_2](\text{PF}_6)_4 \cdot 5\text{H}_2\text{O} \cdot \text{MeCN}$ (2) at 120 K	S5
Table S2 Relevant coordination bond lengths (Å) and angles (°) for $[\text{Fe}^{\text{II}}(\text{L1}^{\text{Me}})_2](\text{PF}_6)_2$ (1) at 150 and 448 K and $[\text{Fe}^{\text{II}}_2(\text{L2}^{\text{C}2})_2](\text{PF}_6)_4 \cdot 5\text{H}_2\text{O} \cdot \text{MeCN}$ (2) at 120 K	S6
Table S3 Intermolecular contacts (Å) for $[\text{Fe}^{\text{II}}(\text{L1}^{\text{Me}})_2](\text{PF}_6)_2$ (1) at 150 and 448 K and $[\text{Fe}^{\text{II}}_2(\text{L2}^{\text{C}2})_2](\text{PF}_6)_4 \cdot 5\text{H}_2\text{O} \cdot \text{MeCN}$ (2) at 120 K	S7
References	S7

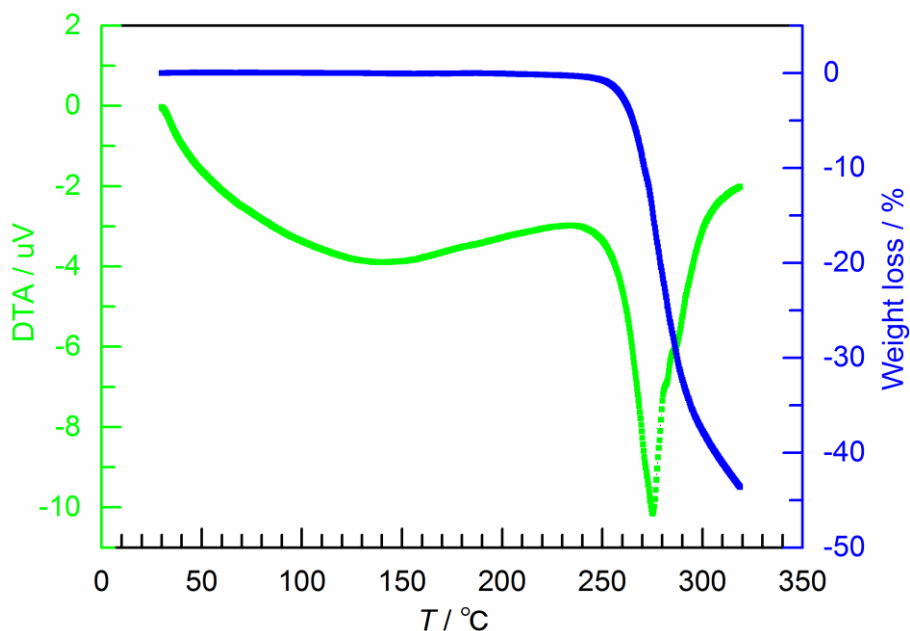


Fig. S1 TG/DTA curves of $[\text{Fe}^{\text{II}}(\text{L1}^{\text{Me}})_2](\text{PF}_6)_2$ (**1**).

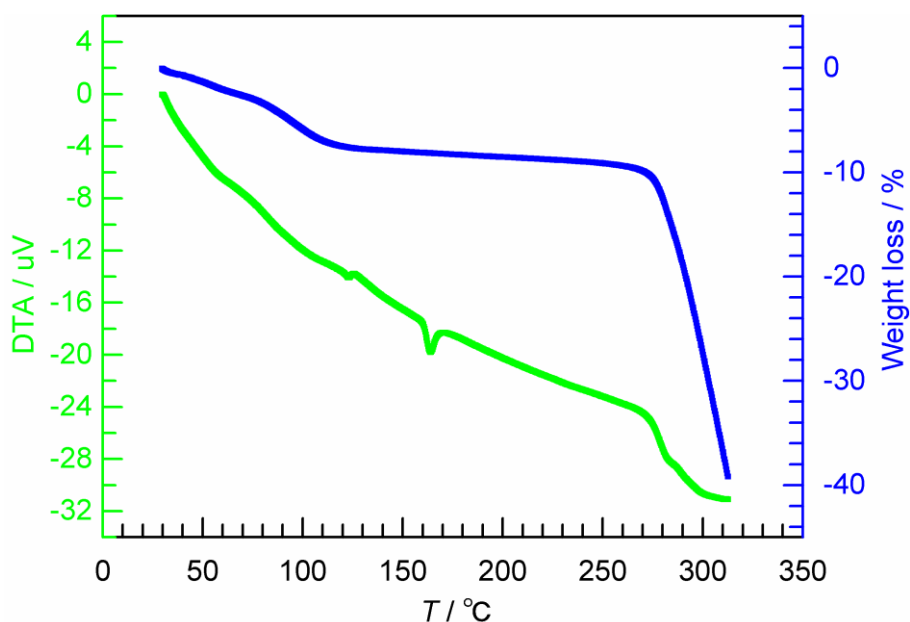


Fig. S2 TG/DTA curves of $[\text{Fe}^{\text{II}}_2(\text{L2}^{\text{C2}})_2](\text{PF}_6)_4 \cdot 5\text{H}_2\text{O} \cdot \text{MeCN}$ (**2**).

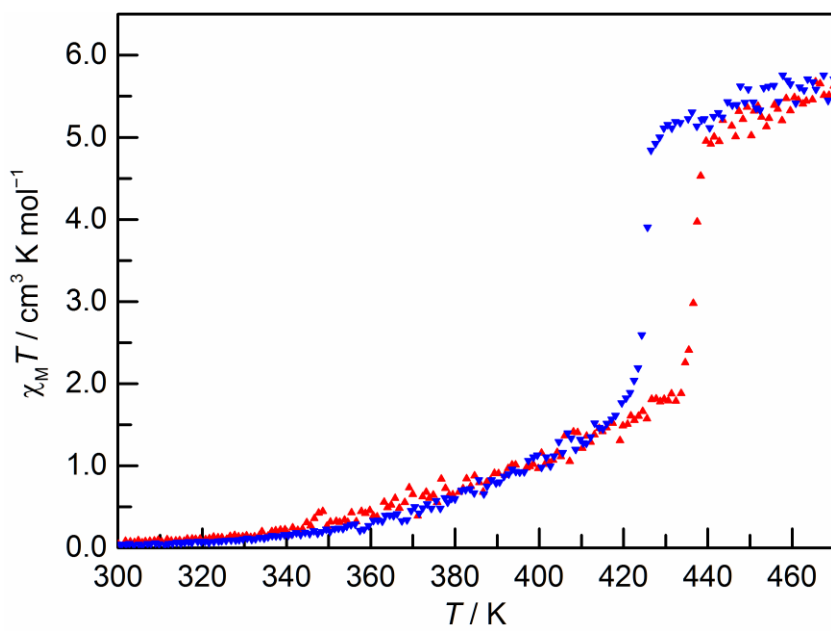


Fig. S3 The magnetic behaviour of desolvated sample **2'** in the form of the $\chi_M T$ vs. T plots. **2'** was warmed from 300 to 470 K (filled triangles; red), and then cooled from 470 to 300 K (filled inverted triangles; blue) at a sweep rate of 1 K min^{-1} .

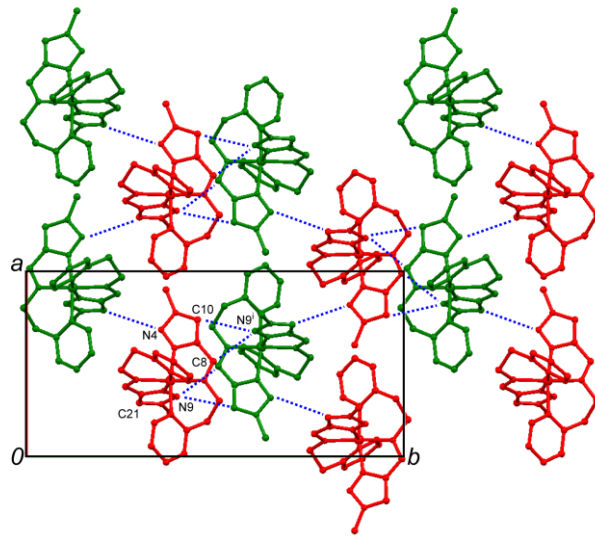


Fig. S4 Heterochiral 2D structure of $[\text{Fe}^{\text{II}}(\text{L1}^{\text{Me}})_2](\text{PF}_6)_2$ (**1**) at 150 K. Δ - $[\text{Fe}^{\text{II}}(\text{L1}^{\text{Me}})_2]^{2+}$ (green) and Λ - $[\text{Fe}^{\text{II}}(\text{L1}^{\text{Me}})_2]^{2+}$ (red) enantiomers are linked alternately via $\text{CH}\cdots\text{N}$ hydrogen bonds (blue dotted line) and enantiomers of same chirality are not directly connected in a 2D layer.

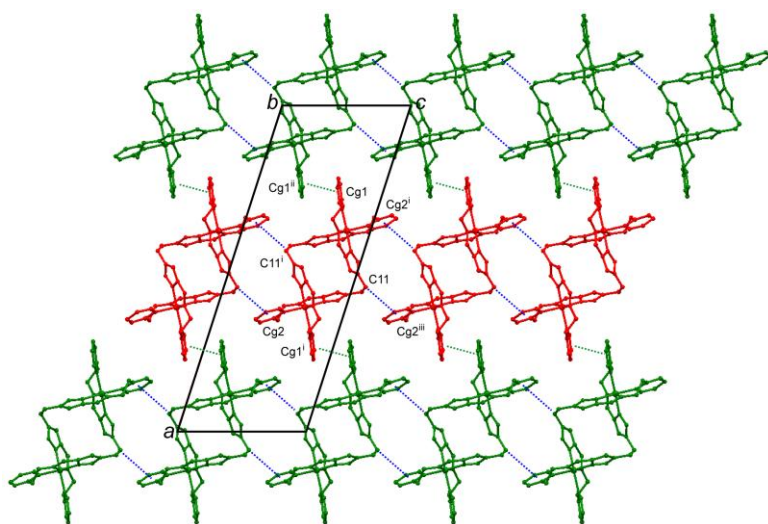


Fig. S5 Heterochiral 2D layer of $[\text{Fe}^{\text{II}}_2(\text{L}2^{\text{C}2})_2](\text{PF}_6)_4 \cdot 5\text{H}_2\text{O} \cdot \text{MeCN}$ (**2**) at 120 K. Green and red colours indicate $\Delta-\Delta-[\text{Fe}^{\text{II}}_2(\text{L}2^{\text{C}2})_2]^{4+}$ and $\Lambda-\Lambda-[\text{Fe}^{\text{II}}_2(\text{L}2^{\text{C}2})_2]^{4+}$ enantiomers, respectively. Homochiral cations are connected by CH/π (blue dotted line) interactions along the *c*-axis ($\Delta-\Delta \cdots \Delta-\Delta \cdots \Delta-\Delta \cdots$ or $\Lambda-\Lambda \cdots \Lambda-\Lambda \cdots \Lambda-\Lambda \cdots$) and cations of opposite chiral pair are linked alternately via $\pi-\pi$ interactions (green dotted line) along the $(a+c)/2$ direction ($\Delta-\Delta \cdots \Lambda-\Lambda \cdots \Delta-\Delta \cdots \Lambda-\Lambda \cdots$).

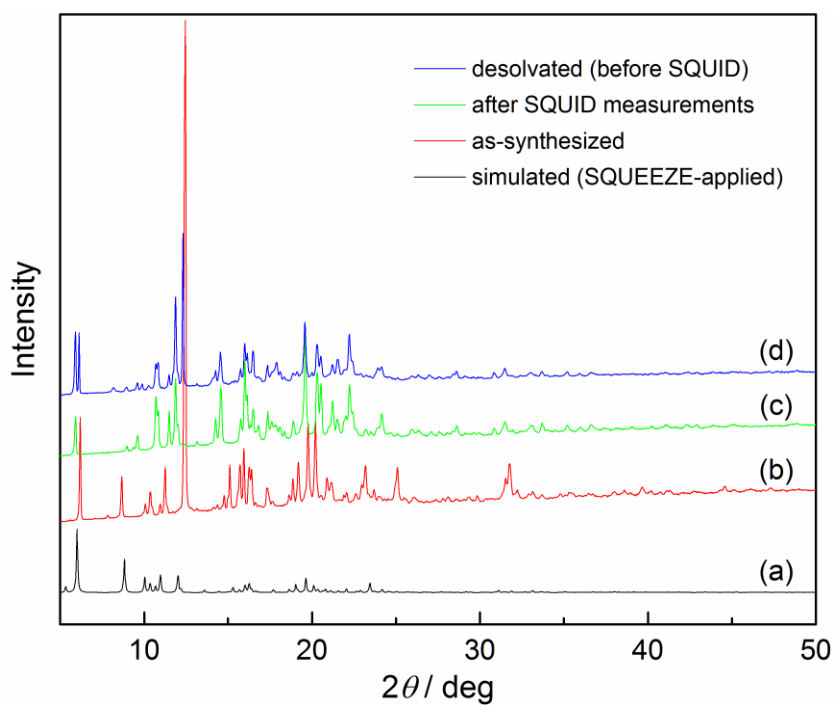


Fig. S6 PXRD patterns of **2** at room temperature in different states: (a) simulated from the SQUEEZE-applied single crystal X-ray data at 120 K; (b) as-synthesized **2**; (c) **2** after SQUID measurements; (d) desolvated **2'** before SQUID measurements.

Table S1 X-ray Crystallographic Data for $[\text{Fe}^{\text{II}}(\text{L1}^{\text{Me}})_2](\text{PF}_6)_2$ (**1**) at 150 and 448 K and $[\text{Fe}^{\text{II}}_2(\text{L2}^{\text{C2}})_2](\text{PF}_6)_4 \cdot 5\text{H}_2\text{O} \cdot \text{MeCN}$ (**2**) at 120 K

Complex	Mononuclear 1		Dinuclear 2 ^a
Temperature	150 K	448 K	120 K
Formula	$\text{C}_{22}\text{H}_{26}\text{N}_{10}\text{P}_2\text{F}_{12}\text{Fe}$		$\text{C}_{46}\text{H}_{51}\text{N}_{21}\text{P}_3\text{F}_{18}\text{Fe}_2$
Formula weight	776.32		1444.68
Crystal system	Monoclinic		Monoclinic
Space group	$P2_1/a$		$C2/c$
a , Å	12.1982(16)	12.647(3)	30.932(8)
b , Å	21.725(3)	22.117(4)	20.020(5)
c , Å	12.2925(16)	12.703(4)	11.614(3)
β , deg	118.8092(12)	119.722(2)	107.907(3)
V , Å ³	2854.4(6)	3085.8(13)	6844(3)
Z	4	4	4
T , K	150(2)	448(2)	120 K(2)
d_{calcd} , g cm ⁻³	1.806	1.671	1.402
μ , mm ⁻¹	0.756	0.699	0.591
R_1 ^b ($ I > 2\sigma(I)$)	0.0404	0.0930	0.0956
wR_2 ^c ($ I > 2\sigma(I)$)	0.0967	0.2253	0.2032
R_1 ^b (all data)	0.0442	0.1291	0.1358
wR_2 ^c (all data)	0.0998	0.2449	0.2215
S	1.064	1.434	1.001
CCDC number	1491569	1491570	1491571

^a The PLATON SQUEEZE program¹ was used to treat regions having highly disordered solvent molecules and counter anions which could not be sensibly modelled in terms of atomic sites. Available void volume is 1386.1 Å³. 473 electrons per unit cell were located and these were assigned to 1 PF₆ and 5 H₂O molecules per complex [473/4 = 119 e per complex; PF₆ (69) + 5 H₂O (10) = 119 electrons].

^b $R_1 = \sum |F_O| - |F_C| | / \sum |F_O|$.

^c $wR_2 = [\sum w(|F_O|^2 - |F_C|^2)^2 / \sum w|F_O|^2]^{1/2}$.

Table S2 Relevant coordination bond lengths (Å) and angles (°) for $[\text{Fe}^{\text{II}}(\text{L1}^{\text{Me}})_2](\text{PF}_6)_2$ (**1**) at 150 and 448 K and $[\text{Fe}^{\text{II}}_2(\text{L2}^{\text{C}2})_2](\text{PF}_6)_4 \cdot 5\text{H}_2\text{O} \cdot \text{MeCN}$ (**2**) at 120 K

Complex	Mononuclear 1		Dinuclear 2
Temperature	150 K	448 K	120 K
Bond Lengths (Å)			
Fe(1)-N(1)	2.0170(16)	2.141(4)	2.017(7)
Fe(1)-N(2)	1.9718(16)	2.085(4)	1.953(5)
Fe(1)-N(3)	1.9915(16)	2.140(4)	1.926(5)
Fe(1)-N(6) ⁱ	2.0196(17)	2.107(5)	2.029(4)
Fe(1)-N(7) ⁱ	1.9814(17)	2.098(4)	1.952(6)
Fe(1)-N(8) ⁱ	1.9954(16)	2.167(4)	1.949(5)
Average Fe-N	1.996	2.123	1.971
Bond Angles (deg)			
N(1)-Fe-N(2)	91.04(6)	88.23(16)	91.8(2)
N(1)-Fe-N(3)	171.42(7)	165.23(16)	172.8(2)
N(1)-Fe-N(6) ⁱ	88.80(7)	89.68(17)	90.6(2)
N(1)-Fe-N(7) ⁱ	93.40(6)	97.69(16)	98.0(3)
N(1)-Fe-N(8) ⁱ	88.54(7)	88.47(16)	91.7(2)
N(2)-Fe-N(3)	80.43(7)	77.07(15)	81.14(19)
N(2)-Fe-N(6) ⁱ	95.73(7)	101.69(17)	96.29(18)
N(2)-Fe-N(7) ⁱ	171.84(7)	167.32(18)	167.5(3)
N(2)-Fe-N(8) ⁱ	93.52(7)	92.73(16)	91.94(18)
N(3)-Fe-N(6) ⁱ	93.00(7)	94.62(16)	88.89(19)
N(3)-Fe-N(7) ⁱ	94.95(6)	96.47(15)	89.2(2)
N(3)-Fe-N(8) ⁱ	90.99(7)	90.81(15)	89.9(2)
N(6) ⁱ -Fe-N(7) ⁱ	91.21(7)	89.60(18)	91.4(2)
N(6) ⁱ -Fe-N(8) ⁱ	170.42(7)	165.40(16)	171.4(2)
N(7) ⁱ -Fe-N(8) ⁱ	79.77(7)	76.31(18)	80.1(2)
Σ^a	46.3	64.7	42.5
\varTheta^b	132.8	208.8	133.7

^a Σ = the sum of $|90 - \varphi|$ for the 12 *cis* N-Fe-N angles in the octahedral coordination sphere.²

^b \varTheta = the sum of $|60 - \theta|$ for the 24 N-Fe-N angles describing the trigonal twist angles.³

Symmetry operation relevant only to **2**: (i), $1 - x, y, 3/2 - z$.

Table S3 Intermolecular contacts (\AA) for $[\text{Fe}^{\text{II}}(\text{L1}^{\text{Me}})_2](\text{PF}_6)_2$ (**1**) at 150 and 448 K and $[\text{Fe}^{\text{II}}_2(\text{L2}^{\text{C2}})_2](\text{PF}_6)_4 \cdot 5\text{H}_2\text{O} \cdot \text{MeCN}$ (**2**) at 120 K

Complex	Temp.	C-H \cdots X or X \cdots X	$d(\text{C-H})$	$d(\text{H}\cdots\text{X})$	$d(\text{C}\cdots\text{X})$	$\langle(\text{C-H}\cdots\text{X})\rangle$
Mononuclear 1	150 K	C(8)-H(9) \cdots N(9) ⁱ	0.950	2.648	3.393(2)	135.63
		C(10)-H(10) \cdots N(9) ⁱ	0.950	2.905	3.527(3)	124.16
		C(21)-H(23) \cdots N(4) ⁱⁱ	0.950	2.687	3.525(3)	147.47
	448 K	C(8)-H(9) \cdots N(9) ⁱ	0.930	2.863	3.633(6)	141.02
		C(21)-H(23) \cdots N(4) ⁱⁱ	0.930	2.735	3.601(8)	155.46
Dinuclear 2	120 K	Cg1 ^c \cdots Cg1 ⁱⁱ			3.937(4)	
		C(1) \cdots C(4) ⁱⁱ			3.900(9)	
		C(2) \cdots C(4) ⁱⁱ			3.676(13)	
		C(2) \cdots C(5) ⁱⁱ			3.906(11)	
		C(3) \cdots C(4) ⁱⁱ			3.642(14)	
		C(3) \cdots C(5) ⁱⁱ			3.625(12)	
		C(3) \cdots Cg1 ⁱⁱ			3.730	
		C(4) \cdots C(4) ⁱⁱ			3.776(11)	
		C(4) \cdots C(5) ⁱⁱ			4.010(9)	
		C(4) \cdots Cg1 ⁱⁱ			3.604	
		C(11)-H(11) \cdots Cg2 ^{d,iii}	0.990	3.681	3.991	101.09
		C(11)-H(12) \cdots Cg2 ⁱⁱⁱ	0.989	3.452	3.991	116.44

^c Cg1 = Centroid of the N1-C1-C2-C3-C4-C5 ring.

^d Cg2 = Centroid of the N6-C12-C13-C14-C15-C16 ring.

Symmetry operations for **1**: (i), $1 - x, 1 - y, 1 - z$; (ii), $-1/2 + x, 1/2 - y, z$.

Symmetry operations for **2**: (ii), $1/2 - x, 1/2 - y, 1 - z$; (iii), $x, y, 1 + z$.

References

- 1 A. L. Spek, *Acta Cryst.*, 2015, **C71**, 9–18.
- 2 P. Guionneau, M. Marchivie, G. Bravic, J.-F. Létard and D. Chasseau, *Top. Curr. Chem.*, 2004, **234**, 97–128.
- 3 M. Marchivie, P. Guionneau, J.-F. Létard and D. Chasseau, *Acta Cryst.*, 2005, **B61**, 25–28.